Quest Journals
Journal of Architecture and Civil Engineering
Volume 7 ~ Issue 4 (2022) pp: 39-44
www.questjournals.org

Research Paper

Deflection Equations for Beams Confined With FRP Tubes

Hamdy M. Mohamed
Associate Professor, College of Engineering, Applied Science University (ASU), Bahrain

ABSTRACT
This study presents experimental and theoretical programs conducted to study the flexural behaviour of reinforced concrete-filled FRP tubes (RCFFTs) beams tested. Pure flexural tests have been conducted on 3 RCFFT and RC beams of a total length 2000 mm with constant diameter 213 mm. The test variables were the type of internal reinforcements (steel or GFRP bars), the FRP tube thickness and the type of transverse reinforcements (spiral steel or FRP tubes). The test results indicated that using FRP tubes changed the failure modes of RCFFT beams to flexural-tension failure modes. The prevailing flexural modes of failure were the tensile rupture of the FRP tube in the longitudinal direction associated with rupture of the reinforcing bars in the tension side. An analytical investigation to examine the validity of the available design provisions for predicting the load-deflection response of RCFFT is conducted. The effective moments of inertia of the tested beams are analyzed using the different available code, manuals and design guidelines equations. The results of the analysis are compared with the experimental values. It has been found that the predicted tension stiffening for steel or FRP-RCFFT beams using the conventional equations (steel or FRP-RC member) is underestimated and hence the predicted deflections are overestimated.
KEYWORDS: *Fibre Reinforced Polymers, FRP Structural Shapes, FRP poles, Filament Winding.*

***R**eceived 12 Apr, 2022; **R**evised 26 Apr, 2022; **A**ccepted 28 Apr, 2022 © The author(s) 2022.*
P**ublished with open access at **www.questjournals.org

I. INTRODUCTION

Corrosion of steel reinforcement causes continual degradation to the infrastructures in worldwide and it has prompted the need for challenges to those involved with reinforced concrete structures. In the last decade, considerable efforts have been made to apply fibre-reinforced polymers (FRP) composites in the construction industry, and recently, structural applications of FRP composites started to appear in civil infrastructure systems. FRP composite materials have been used as internal and external reinforcement in the field of civil engineering constructions. It has been used as internal reinforcement for beams, slabs and pavements (), and also as external reinforcement for strengthening different structures. Recently, the use of FRP tubes as structurally integrated stay-in-place forms for concrete members, such as beams, columns, bridge piers, piles and fender piles has emerged as an innovative solution to the corrosion problem (Mohamed and Masmoudi 2010).. In such integrated systems, the FRP tubes may act as a permanent form, often as a protective jacket for concrete, and especially as external reinforcement in the primary and secondary directions such as for confinement. Furthermore, the use of concrete filled-FRP tubes (CFFTs) technique is predicated on performance attributes linked to their high strength-to-weight ratios, expand the service life of structures, enhance corrosion resistance, and potentially high durability.

II. RESEARCH METHODOLOGY

The test matrix included five beams, one conventional reinforced concrete (RC) circular beams without spiral reinforcement and one RC beam with spiral reinforcement, while the remaining three specimens were RCFFTs. The beam specimens were reinforced with steel or glass FRP bars with the same reinforcement ratio, 0.76%. Table 1 shows the details of RC and RCFFTs beams including their identification, height, diameter and type of internal reinforcements. The specimens were identified by codes listed in the first column of Table 1. The identifications CO and COS are used for control conventional RC beams without and with spiral reinforcement, respectively. The terms D or E indicate the type of the used FRP tube for the beam. The second

letters indicate the type of flexural reinforcement, whereas, S or G means steel or glass FRP bars, respectively, was used for the specimen. The term N is used to indicate the type of concrete used to cast the specimens.

The FRP tubes were cut to the proper length (2.00 m), using saw and then were cleaned and dried carefully. The FRP tubes provided the formwork for beam specimens. The control specimens were prepared for vertical casting using stiff cardboard tubes. The cardboard tubes were attached with four vertical stiffeners using wood plate of 50 x 30 mm, cross section distributed at the perimeter of the tube. Reinforcement cages with different configuration were constructed from glass FRP and steel bars. The rebar cage was designed to have an outside diameter of 193 mm, allowing for 10 mm clear spacing on all perimeters of the FRP tubes, which has a 213 mm internal diameter. The cages of the RCFFT specimens had six longitudinal bars (glass FRP bars or steel bars). The longitudinal bars were held in its positions at equal intervals using three hoop steel stirrup (3.4 mm diameter) at the two ends and middle length of the cages. Figure 1 shows the typical steel and glass FRP cages which had been used to reinforce the RCFFT and control beam specimens.

Figure 1: Typical steel and glass FRP cages for RC and RCFFT beams

Table 1: Test matrix and details of beam specimens.

Tube type	Diameter (D=mm)	Shear reinforcement	4t/D%	Flexural reinforcement	Internal reinforcement ratio	Concrete strength (MPa)
CO-S-N	203	---	-	Steel bars		
COS-S-N	203	Steel spiral	-	Steel bars		
D-S-N	213	Tube D	4.5	Steel bars	3.65 (6 ϕ 15)	30
D-G-N	213	Tube D	4.5	GFRP bars		
E-G-N	213	Tube E	12.6	GFRP bars		

2.3 Instrumentation and test setup

Electrical resistance strain gauges were attached to the reinforcing bars, concrete surface and FRP tube surface. In each beam, two electrical strain gauges of type KFG-6-120-C1-11L3M3R and gauge length 6 mm were bonded on the longitudinal reinforcing bars at mid-span to measure tensile strains. In addition, two electrical strain gauges of length 67 mm were bonded on the top surface of the RC beams at mid-span to measure the concrete compressive strains. The strain gages were distributed evenly around the section at 60° angles. The deflections were measured using three LVDTs at the mid-span and at each quarter-span to monitor the deflection profile along the beams. Two high-accuracy LVDTs (± 0.001 mm) were installed at the mid-span to measure the crack width. Also, one LVDT was attached at each support, to measure beam end rotations.

The specimens were tested in four-point bending over a simply supported clear span of 1920 mm, see Figure 2. The load was transferred from the actuator to the tested beam at two points through a steel spreader I-beam applied on the round surface of the beams through curved loading plates on one-third diameter of the beam. A roller support was obtained by placing a steel cylinder between two steel flat plates. A pin support was obtained by using specially adapted steel I-beam. The upper plate of the I-beam had spherical groove and the plate was supported on the web plate which had a spherical end to house the plate and allow the rotation. During the test, the load was monotonically applied at a stroke controlled rate of 0.8 mm/minute using a 500 kN closed-loop MTS actuator. The applied load was measured by the internal load cell on the actuator.

Load-deflection behavior

The applied load versus mid-span deflection relationships of the five beams are presented in Figure 3. The influence of the confinement using steel spiral or FRP tubes of the three beams (CO-SN, COS-SN and DSN) reinforced internally with steel bars is shown in Figure 3. The load-deflection curve was bilinear for the two beams COS-SN and DSN, and linear for the beam CO-SN. The figure shows the elastic-plastic behaviour of the steel-reinforced beams (COS-SN and DSN) and their eventual failure at large deflection. Also, the figure shows the brittle shear failure of the beam without transverse reinforcement, (beam CO-SN). The figure indicates that the beam confined by FRP tube (DSN) experienced lower deflection, higher stiffness and superior strength (55 % higher than the beam reinforced with steel spiral). The initial stiffness and the stiffness after yielding of the Specimen DSN was approximately 61 and 49 %, respectively, higher than that of the beam reinforced with steel spiral. This is attributed to the contribution of the helical fibres of the FRP tubes to provide shear and flexural resistance to the beam, and to confine a much larger concrete cross-sectional area than steel spiral.

The effect of type of the internal reinforcements on the flexural performance of RCFFT beams can be observed through the comparisons of the load-deflection curves of Specimens DSN with DGN, (Figure. 3). Steel and Glass FRP bars with the same cross section area were used to reinforce concrete beams. All the four beam specimens were cast using the same type of the FRP tube, Type D with confinement-reinforcement ratio (4t/D) equal to 4.5 %. Since, FRP reinforcing bars is linear-elastic to failure when loaded in tension and fail in a brittle manner, a ductile steel-like failure does not occur in FRP-reinforced concrete beams. Figure 3 shows the elastic-plastic behaviour of the steel-reinforced beam (DSN) and its failure load at larger deflection as compared with the elastic behaviour of FRP-reinforced beam (DGN). The behaviour of FRP RCFFT beams showed no yielding compared to that of the steel-RCFFT beam. The figures indicate that the beam reinforced with steel bars (DSN) experienced lower deflection, higher stiffness with 64 % higher strength than that of the CFFT beam reinforced with FRP bars (DGN).

The effect of the FRP tube thickness is presented through the load-deflection curves of the specimens (DGN and EGN) in Figure 3. The two beams had identical reinforcement ratio of the GFRP bars. The FRP tube Type E has thickness 6.40 mm, that it is equal to 2.2 times the thickness of the tube Type D, (2.90 mm). The load-deflection profiles for the four beams exhibited similar characteristics. The figure indicates that the beam casted in the tube E (EGN) experienced 22.3 % higher strength than that of beam casted in the tube D (DGN). Also, the RCFFT beams of tube E showed lower deflection than that of beams with tube D, at all load levels. The increase in the strength is attributed to the contribution of the FRP tube in the tensile and compressive strength of the beams in the tension and compression sides, respectively. Also, the increase in the stiffness is attributed to the confinement of the FRP tube to the concrete cores, which in turn reduced the flexural and shear cracks along the longitudinal axis of the beams.

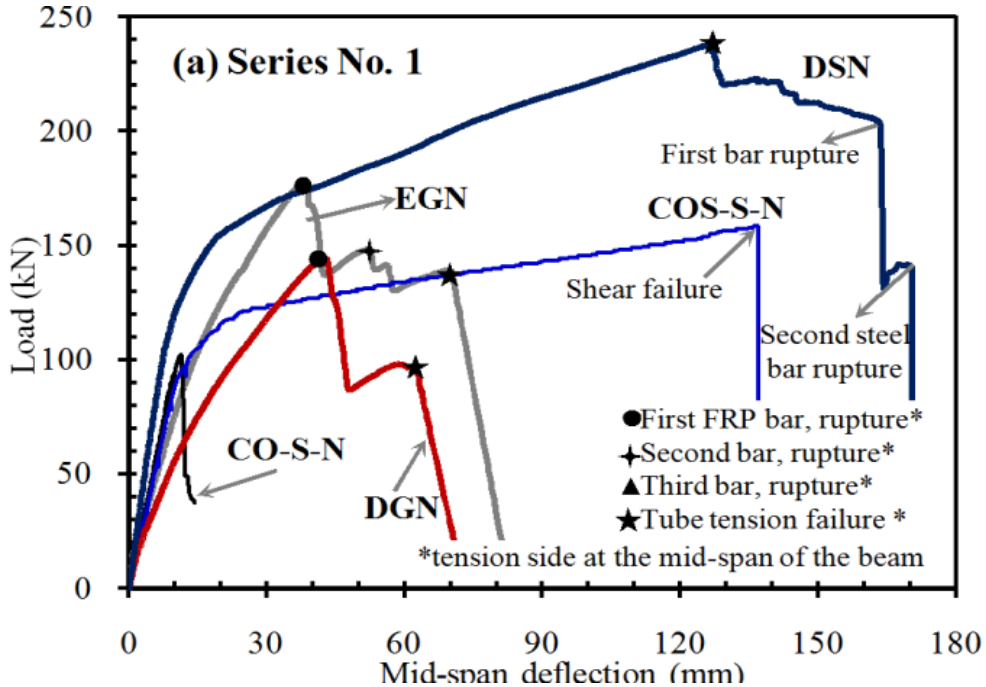

Figure 2: Load–deflection curves of control and CFFT beams.

Evaluation of moment of inertia equations for deflection prediction of RCFFT beams

The values of the experimental moment of inertia I_{exp} for the tested RCFFT beams are determined based on the laboratory-measured applied loads P_{exp} and the corresponding center-span deflections Δ_{exp} using the following equation:

$$I_{exp} = \frac{P_{exp} a}{48 E_c \Delta_{exp}} (3L^2 - 4a^2) \quad \text{Eq 7}$$

A comparison of the experimental I_e / I_g values, which were computed using the recorded deflection data and those predicted using the Branson's equation (ACI 318-08), has been plotted in Figure 6, versus M_a / M_{cr} for the tested steel-RCFFT beams, DSN. It can be seen that Branson's equation gives a response that is obviously too less stiff of these beams. On the other hand, Figure 7 presents experimental and theoretical predictions of I_e / I_g versus M_a / M_{cr} relationships for the four tested FRP-RCFFT beams, DGN and EGN. The theoretical predictions of I_e are determined using five selected equations for FRP-RC beams, which are presented in the previous section, ACI 318-08 (Branson's equation); ACI 440.1R-06; ISIS 2001; Masmoudi et al. 1998; Benmokran et al. 1996.

It has been observed that all the aforementioned equations does not predict deflection well of the FRP-RCFFT beams. All the former equations had been modified to account for the nature of the FRP reinforcement that exhibited larger deformation than the steel reinforcement. However, in case of steel or FRP-RCFFT members, the behaviour under the flexural load is significantly different than that of steel or FRP RC members. Again, this is attributed to the confinement of the concrete core and the axial contribution of the FRP tube which in turn enhances the overall flexural behaviour and improves the tension stiffening of RCFFT beams. Therefore, the tension stiffening predicted for steel or FRP-RCFFT beams using the former equations (steel or FRP-RC member) is underestimated and hence the predicted deflections are overestimated.

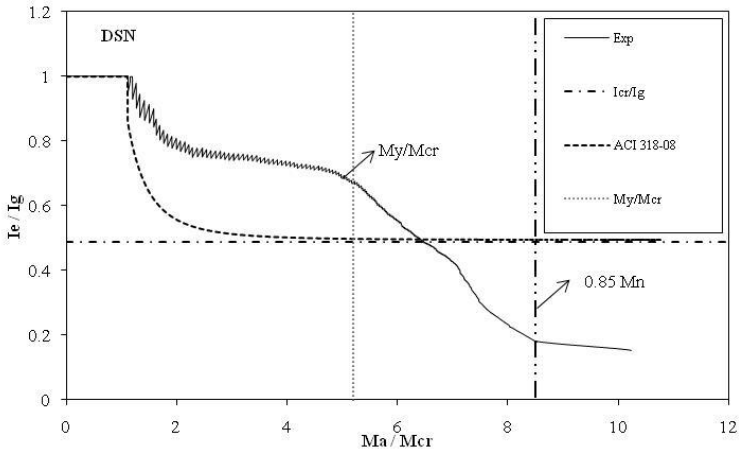

Figure 3: Effective to gross moment of inertia versus M_a / M_{cr}, (Steel-RCFFT beams)

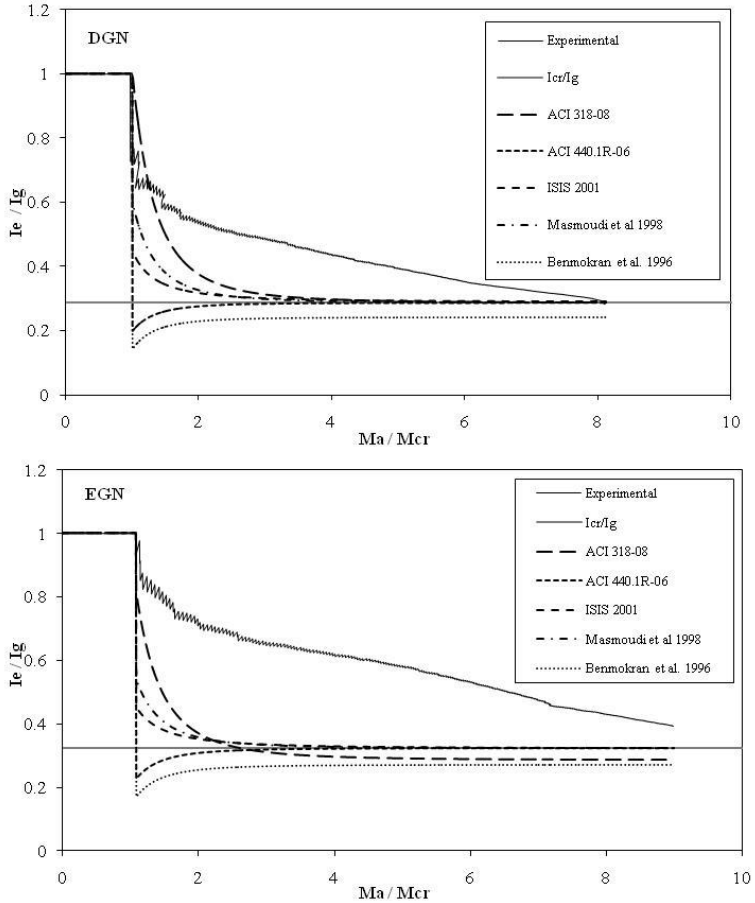

Figure 4: Effective to gross moment of inertia versus M_a / M_{cr}, (FRP-RCFFT beams)

III. Conclusion

The experimental test results indicated that the beams confined by FRP tubes experienced lower deflection, higher cracking load level, higher ductility, higher stiffness and superior strength than the beam reinforced with a spiral-steel. It was found that the confinement provided by the FRP tubes improved the tension stiffening of the tested beams. The experimental results of tested RCFFTs beams in four-point loading bending with varying properties revealed that the current conventional or modified models available in the literature, codes (ACI 318-08; CSA A23.3-04; SAA 2001) and design guidelines (ACI 440.1R-06; ISIS 2001) for predicting the effective moment of inertia of beams reinforced by steel or FRP bars, respectively, over-estimates the deflections in these beams and therefore it needs to be revised.

Acknowledgements

The research reported in this paper was partially sponsored by the Natural Sciences and Engineering Research Council of Canada (NSERC). The authors also acknowledge the contribution of the Canadian Foundation for Innovation (CFI) for the infrastructure used to conduct testing. Special thanks to the manufacturer (FRE Composites, St-André d'Argenteuil, QC, Canada) for providing FRP tubes.

REFERENCES

[1]. American Concrete Institute (ACI). (2008). "Building code requirements for structural concrete." ACI-318-08, Farmington Hills, Mich.

[2]. American Concrete Institute, (ACI). Committee 440, (2003), "Guide for the design and construction of concrete reinforced with FRP bars (ACI 440.1R-03)." Farmington Hills, MI, 42 pp.

[3]. ASTM. (2009). "Standard specification for deformed and plain carbon steel bars for concrete reinforcement." A615/A615M-09, West Conshohocken, Pa.

[4]. Benmokrane, B. Chaallal, O., and Masmoudi, R. (1996). "Flexural response of concrete beams reinforced with FRP reinforcing bars." ACI Struct J., 93(1), 46-55.

[5]. Bischoff, P. H. (2007). "Deflection calculation of FRP reinforced concrete beams based on modification to the existing Branson equation." Journal of Comp for Const, ASCE., 11(1), 4-14.

[6]. Branson, D. E. (1965). "Instantaneous and time-dependent deflections of simple and continuous reinforced concrete beams." HPR Rep. No. 7, Part 1, Alabama Highway Dept., Bureau of Public Roads, Alabama (Dept. of Civil Engineering and Auburn Research Foundation, Auburn Univ., Aug. 1963).

[7]. Canadian Standard Association (CSA). (2004), "Design of concrete structures." CSA standard CAN/CSA-A23.3-04, Rexdale, Ont.
[8]. Cole, B., and Fam, A. (2006) "Flexural load testing of concrete-filled FRP tubes with longitudinal steel and FRP rebar." Journal of Comp for Const, ASCE., 10(2), 161-171.
[9]. Fam, A., Cole, B., and Mandal, S. (2007). "Composite tubes as an alternative to steel spirals for concrete members in bending and shear." Journal Construction and Building Materials., 21, 347–355.
[10]. Gilbert, R. I. (2006). "Discussion of 'Reevaluation of deflection prediction for concrete beams reinforced with steel and fiber reinforced polymer bars." by Peter H. Bischoff. Journal Struct Eng, 132(8), 1328–1330.
[11]. ISIS Canada. (2001). "Reinforcing concrete structures with fibre reinforced polymers." Design Manual No. 3, ISIS Canada, Winnipeg, Manitoba, Canada.
[12]. Mandal S., and Fam, A. (2006). "Modeling of prestressed concrete-filled circular composite tubes subjected to bending and axial loads." Journal of Comp for Const, ASCE., 132(3), 449–459.
[13]. Masmoudi, R., Thériault, M., and Benmokrane, B. (1998). "Flexural behaviour of concrete beams reinforced with deformed fibre reinforced plastic reinforcing rods." ACI Struct J., 95, (6), 665-76.
[14]. Mirmiran, A., Shahawy, M., El Khoury, C. and Naguib, W. (2000). "Large beam-column tests on FRP-filled composite tubes." ACI Struct J., 97(2), 268–276.
[15]. Mohamed, H., and Masmoudi, R. (2008). "Compressive behaviour of reinforced concrete filled FRP tubes." ACI Special Publications, SP-257-6, 91-108.
[16]. Mohamed H. M. (2010). "Axial and flexural behavior of reinforced concrete-filled fiber reinforced polymer tubes: experimental and theoretical studies." Ph.D. thesis. University of Sherbrooke.
[17]. Mohamed, H., and Masmoudi, R. (2010). "Axial load capacity of reinforced concrete-filled FRP tubes columns: experimental versus theoretical predictions." Journal of Comp for Const, ASCE., 14(2), 1-13.
[18]. Standards Association of Australia (SAA). (2001). "Australian standard for concrete structures." AS 3600-2001, SAA, Sydney, Australia.
[19]. Toutanji, H. A., and Deng, Y. (2003). "Deflection and crack-width prediction of concrete beams reinforced with glass FRP rods." Construction and Building Materials., 17, 69-74.
[20]. Yost, J. R., Gross, S. P. and Dinehart, D. W. (2003). "Effective moment of inertia for glass fiber-reinforced polymer-reinforced concrete beams." ACI Struct J., 100(6), 732-739.